

## **Biocorrosion and Surface Wettability of Ni-free Zr-Based Bulk Metallic Glasses**

Amin Monfared<sup>1,2</sup>, Shahab Faghihi<sup>1</sup>, Hassan Karami<sup>3,\*</sup>

<sup>1</sup> Tissue Engineering and Biomaterials Division, National Institute of Genetic Engineering and Biotechnology (NIGEB), Tehran, Iran, P.O. box 14155-6343

<sup>2</sup> Faculty of Biomedical Engineering, Amirkabir University of Technology, Tehran, Iran, P.O. Box: 15875-4413

<sup>3</sup> Nano Research Laboratory, Department of Chemistry, Payame Noor University, 19395-4697, Tehran, I.R. of Iran

\*E-mail: [karami\\_h@yahoo.com](mailto:karami_h@yahoo.com)

*Received:* 21 April 2013 / *Accepted:* 13 May 2013 / *Published:* 1 June 2013

---

Owing to the amorphous structure, bulk metallic glasses (BMGs) demonstrate attractive properties for potential biomedical applications. In this study, three Ni-free Zr-based BMGs including  $Zr_{60}Cu_{22.5}Fe_{7.5}Al_{10}$ ,  $Zr_{60}Cu_{20}Fe_{10}Al_{10}$  and  $Zr_{60}Ti_6Cu_{19}Fe_5Al_{10}$  were fabricated by suction casting technique. The biocorrosion behaviors of the BMGs in phosphate buffer solution (PBS, pH=7.4) at 37°C were investigated and compared to crystalline biomaterials including Ti-6Al-4V and 316L stainless steel as controls. The corroded surface morphologies and compositions of the BMGs were evaluated by scanning electron microscopy (SEM) and energy dispersive X-ray (EDX), respectively. Surface wettability of the samples was determined by static contact angle measurement at room temperature using deionized water. It was found that  $Zr_{60}Cu_{20}Fe_{10}Al_{10}$  BMG showed a higher passive region compared to that of  $Zr_{60}Cu_{22.5}Fe_{7.5}Al_{10}$ , however these BMGs exhibited lower pitting corrosion resistance compared to crystalline biomaterials. However, titanium element addition to the Zr-Cu-Al-Fe BMGs exhibited a significant increase in the passive region of the polarization curve and a considerable pitting corrosion resistance improvement. Contact angle measurements showed that all BMGs were smaller than the Berg limit ( $\theta = 65^\circ$ ), i.e. they were hydrophilic, which may enhance cell adhesion of the BMGs in biomedical applications.

---

**Keywords:** Bulk metallic glasses; Biocorrosion; Wettability; Biomedical application

### **1. INTRODUCTION**

Metals have extensive application as biomedical materials in fabrication of prosthesis such as artificial joints, stents and dental implants. Stainless steels, titanium and cobalt-based alloys are the

most commonly used metallic biomaterials. However, they suffer from several drawbacks during their applications such as stress shielding, aseptic loosening, corrosion-fatigue failure and chronic inflammation [1-3]. Considering the significance of metallic materials in fabrication of artificial joints and implants there is a need for new materials with enhanced mechanical and chemical properties having sufficient biocompatibility to endure cyclic loads and corrosive body environment.

Amorphous metallic alloys (metallic glasses) with unique mechanical and chemical properties and attractive processing capabilities are promising candidate materials for achieving these goals. Bulk metallic glasses (BMGs) are a revolutionary group of alloys that unlike crystalline materials possess an amorphous microstructure [4,5]. A number of BMGs, especially Zr-based alloys, have superior strength (GPa), high elastic strain limit (2%) and relatively low Young's modulus (50–100 GPa) [6-9]. It is demonstrated that for a given strength requirement a glassy alloy exhibits a significantly lower modulus than any of the conventional crystalline metallic biomaterials which implies better load transfer to the surrounding bone and the potential for appeasing stress-shielding [6-9]. Wear resistance of bulk metallic glasses were found to exceed that of ceramics with the same level of hardness. This could be a great asset in load-bearing bio-implant applications as it could prevent wear debris production and reduce the risk of aseptic loosening [8-10]. Another significant characteristic of metallic glasses is their viscoplastic flow which allows their thermoplastic forming (TPF) process for tissue engineering applications [7,11,12].

Most of the Zr-based BMGs developed to date contain Ni element which is usually blamed for the occurrence of an allergy and has antiproliferative effects on cell cultures [13]. Therefore, it is anticipated to prepare Ni-free or, at least, Ni-reduced Zr-based BMGs in order to further improve their biocompatibility. It has been reported that BMGs in Zr-Cu-Fe-Al system have an excellent glass forming ability that increase their potential for structural applications [14]. In this study we fabricated Ni-free Zr-based bulk amorphous alloys in Zr-Cu-Fe-Al system having the compositions of  $Zr_{60}Cu_{22.5}Fe_{7.5}Al_{10}$ ,  $Zr_{60}Cu_{20}Fe_{10}Al_{10}$  and Ti-bearing composition of  $Zr_{60}Ti_6Cu_{19}Fe_5Al_{10}$ .

In the present study the corrosion behaviors of Ni-free BMGs in Zr-Cu-Fe-Al system is investigated. The test was performed in phosphate buffer solution (PBS) as electrolyte at 37°C and the corroded surface morphology and corrosion products were characterized by scanning electron microscopy (SEM) and energy dispersive X-ray (EDX), respectively. The results were compared with 316L stainless steel and Ti-6Al-4V, as controls. Whereas Cell attachment/adhesion was found to be specially related to surface wettability, the characterization of the wettability of the glassy alloys was evaluated by the sessile drop contact angle method with deionized water.

## 2. EXPERIMENTAL PROCEDURE

The alloy ingots with nominal compositions of  $Zr_{60}Cu_{22.5}Fe_{7.5}Al_{10}$ ,  $Zr_{60}Cu_{20}Fe_{10}Al_{10}$  and  $Zr_{60}Ti_6Cu_{19}Fe_5Al_{10}$  (%) were prepared by arc melting of the pure elements mixture in an argon atmosphere. Pure titanium was melted prior to the preparation of the master ingot to absorb the oxygen atoms in the furnace as it is detrimental to the glass formability. The ingot alloys were remelted several times to ensure the compositional homogeneity. The melted ingots were casted into cylindrical rods

with a diameter of 3 mm and length of about 20 mm using suction casting copper mold technique. X-ray diffraction was performed to verify the amorphous structure of the samples using Cu  $k_{\alpha}$  radiation operated at 40 kV and 20mA with the  $2\theta$  range from  $20^{\circ}$  to  $80^{\circ}$  (X-Pert-Pro 2001 diffractometer).

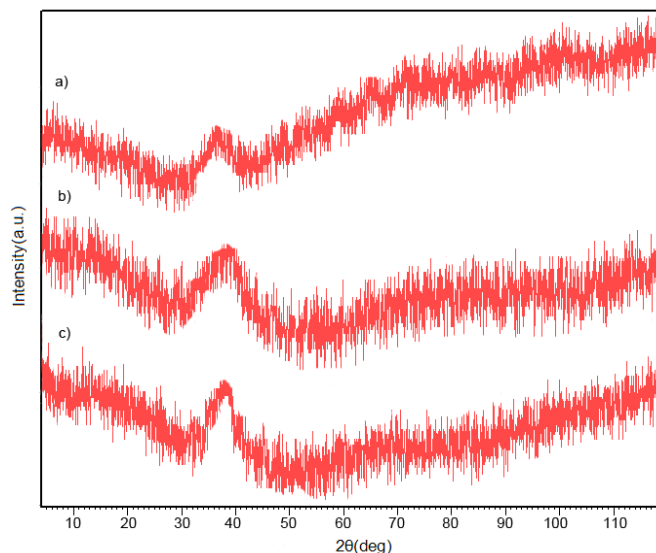
The test samples for corrosion experiment were prepared by cutting the cylindrical BMG rods in slices having 3 mm diameter and 10 mm of thickness. They were closely sealed with epoxy resin in a way to leave a cross-section area of about  $7 \text{ mm}^2$ . Prior to the test, the exposed surface area of each specimen was polished to a 600-grit SiC surface finish, cleaned with acetone, sonicated in distilled water bath and dried in air at about 1 h prior to any electrochemical tests. The electrochemical behavior of BMG alloys were studied by polarization curves in a three-electrode cell at  $37^{\circ}\text{C}$ . The distance between reference and working electrodes was fixed throughout the test. The phosphate buffered saline solution (PBS) was used as electrolyte in order to simulate the corrosive body environment. The anodic polarization curves of the specimens were recorded at a potential sweep rate of  $1 \text{ mV/s}$  when the open circuit potential became steady after immersion in PBS for about 30 min. The Ti-6Al-4V and 316L stainless steel samples were prepared with the same method described above and used as controls. SEM and EDX analyses were used to investigate the morphology and chemical compositions of corroded surfaces of the specimens, respectively.

Surface wettability of the samples was evaluated by a contact angle measurement system (OCA 15 plus, Dataphysics) equipped two CCD color cameras and image analysis software (ImageJ). The surface of each sample was polished to a 600-grit SiC surface finish and cleaned in an ultrasonic bath with ethanol, acetone and distilled for 20 min. The water contact angles were measured 10 seconds after deionized water droplet deposition. Repetitive measurements were carried out on quintuplicate samples ( $n = 5$ ) for each group.

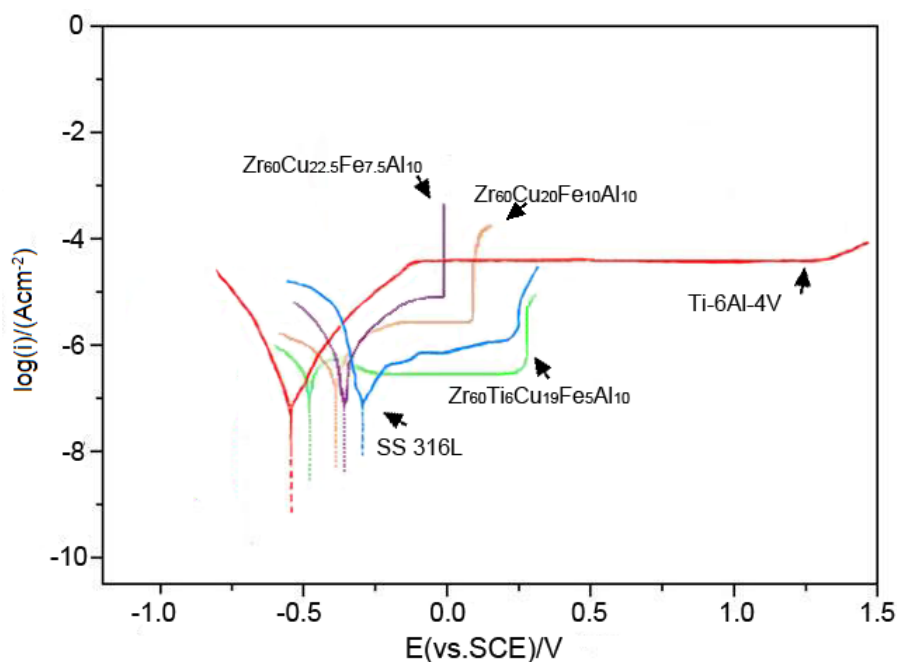
### 3. RESULTS AND DISCUSSIONS

Figure 1 shows X-ray diffraction patterns of Zr-based BMGs. All samples displayed broad peak around  $2\theta = 40^{\circ}$  which is an amorphous structure characteristic. No other detectable diffraction peak from any crystalline phase is visible within the sensitivity of the XRD measurement.

Fig. 2 shows the anodic polarization curves of three Zr-based BMGs in PBS solution at  $37^{\circ}\text{C}$ . The results of 316L stainless steel and Ti-6Al-4V alloy are also presented for comparison. The Table 1 presents the electrochemical information such as  $E_{\text{corr}}$  (corrosion potential),  $i_{\text{corr}}$  (corrosion current density),  $E_{\text{pit}}$  (pitting potential) which are extracted from the polarization curves. As demonstrated in the curves,  $\text{Zr}_{60}\text{Cu}_{22.5}\text{Fe}_{7.5}\text{Al}_{10}$  and  $\text{Zr}_{60}\text{Cu}_{20}\text{Fe}_{10}\text{Al}_{10}$  BMGs demonstrated spontaneous passivation behavior in PBS with a wide passive region and low passive current density. This is an indication for a good corrosion resistance [15,16]. The passive current density of  $\text{Zr}_{60}\text{Cu}_{22.5}\text{Fe}_{7.5}\text{Al}_{10}$  BMG was comparable to that of Ti-6Al-4V alloy and lower than 316L stainless steel and the other BMGs. The lower passive current density was probably due to the formation of a highly uniform and protective passive film on the exposed surface  $\text{Zr}_{60}\text{Cu}_{22.5}\text{Fe}_{7.5}\text{Al}_{10}$  BMG [16,17].



**Figure 1.** X-ray diffraction patterns of (a)  $\text{Zr}_{60}\text{Cu}_{22.5}\text{Fe}_{7.5}\text{Al}_{10}$ , (b)  $\text{Zr}_{60}\text{Cu}_{20}\text{Fe}_{10}\text{Al}_{10}$  and (c)  $\text{Zr}_{60}\text{Ti}_6\text{Cu}_{19}\text{Fe}_5\text{Al}_{10}$  as-cast rods.



**Figure 2.** Anodic polarization curves of Ni-free Zr-based BMGs as well as Ti-6Al-4V and 316L SS samples.

In contrast,  $\text{Zr}_{60}\text{Cu}_{20}\text{Fe}_{10}\text{Al}_{10}$ , that has lower Cu content and higher Fe content, showed a wider passive region compared to the 316L stainless steel sample with a relatively high passive current density. Results indicated that both  $\text{Zr}_{60}\text{Cu}_{22.5}\text{Fe}_{7.5}\text{Al}_{10}$  and  $\text{Zr}_{60}\text{Cu}_{20}\text{Fe}_{10}\text{Al}_{10}$  BMGs showed lower corrosion current density ( $2.01$  and  $2.64 \text{ mA/m}^2$  respectively) than that of  $\text{Zr}_{55}\text{Al}_{10}\text{Cu}_{30}\text{Ni}_5$  BMG ( $\sim 5 \text{ mA/m}^2$ ) [15] that could be related to the formation of a highly uniform and protective passive film on the surface of Ni-free Zr-based BMGs [15-17]. The  $E_{\text{pit}} - E_{\text{corr}}$  value for  $\text{Zr}_{60}\text{Cu}_{20}\text{Fe}_{10}\text{Al}_{10}$  BMG was

higher than that of  $Zr_{50}Cu_{43}Al_7$  and  $Zr_{55}Al_{10}Ni_5Cu_{30}$  BMGs being 0.465 V, 0.388 V and 0.349 V, respectively [15,18].

In comparison with BMG samples, Ti-6Al-4V alloy showed a negative shift (-0.55 V) in polarization curve that it indicates a more active state of the Ti-6Al-4V alloy surface [19].

**Table 1.** Mean corrosion parameters derived from anodic polarization curves

Composition	$E_{corr}$ (V)	$i_{corr}$ ( $A/Cm^2 \cdot 10^{-7}$ )	$E_{pit}$ (V)	$E_{pit}-E_{corr}$ (V)
$Zr_{60}Cu_{22.5}Fe_{7.5}Al_{10}$	-0.37	2.01	-0.05	0.325
$Zr_{60}Cu_{20}Fe_{10}Al_{10}$	-0.39	2.64	0.07	0.465
$Zr_{60}Ti_6Cu_{19}Fe_5Al_{10}$	-0.42	2.34	0.28	0.700
SS 316L	-0.30	2.17	0.17	0.472
Ti-6Al-4V	-0.55	2.05	1.18	1.730

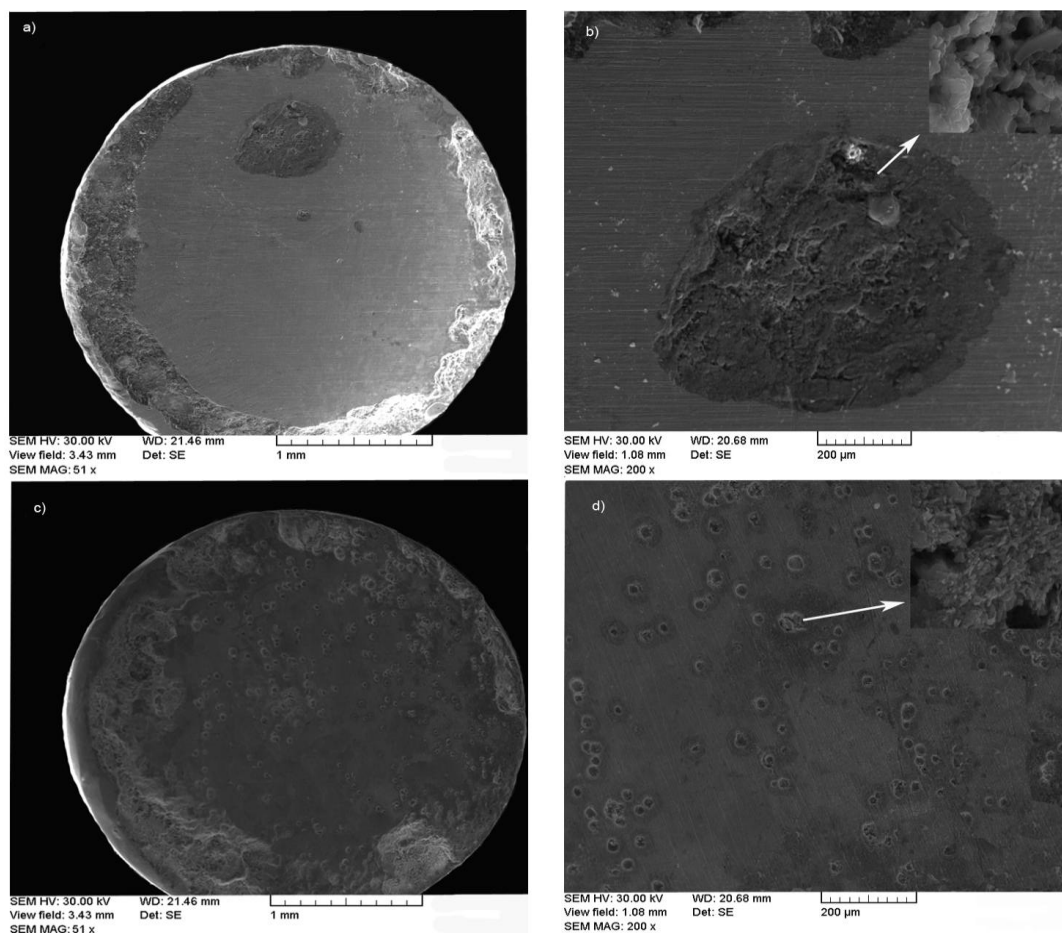


**Figure 3.** SEM images of corroded surface morphology of (a,b)  $Zr_{60}Cu_{20}Fe_{10}Al_{10}$  BMG and (c,d)  $Zr_{60}Ti_6Cu_{19}Fe_5Al_{10}$  BMG.

However, Zr-Cu-Fe-Al BMGs samples demonstrated low  $E_{\text{pit}} - E_{\text{corr}}$  values that indicate they are susceptible to the pitting corrosion when compared to Ti-6Al-4V alloy.

It is reported that Additives of other valve-metals components like Ti and Nb can improve the passive film properties and thus, lead to a certain improvement of the pitting resistance [20,21]. Therefore, we selected Ti element and investigated effect of the addition of titanium to Zr-Cu-Fe-Al BMG system.

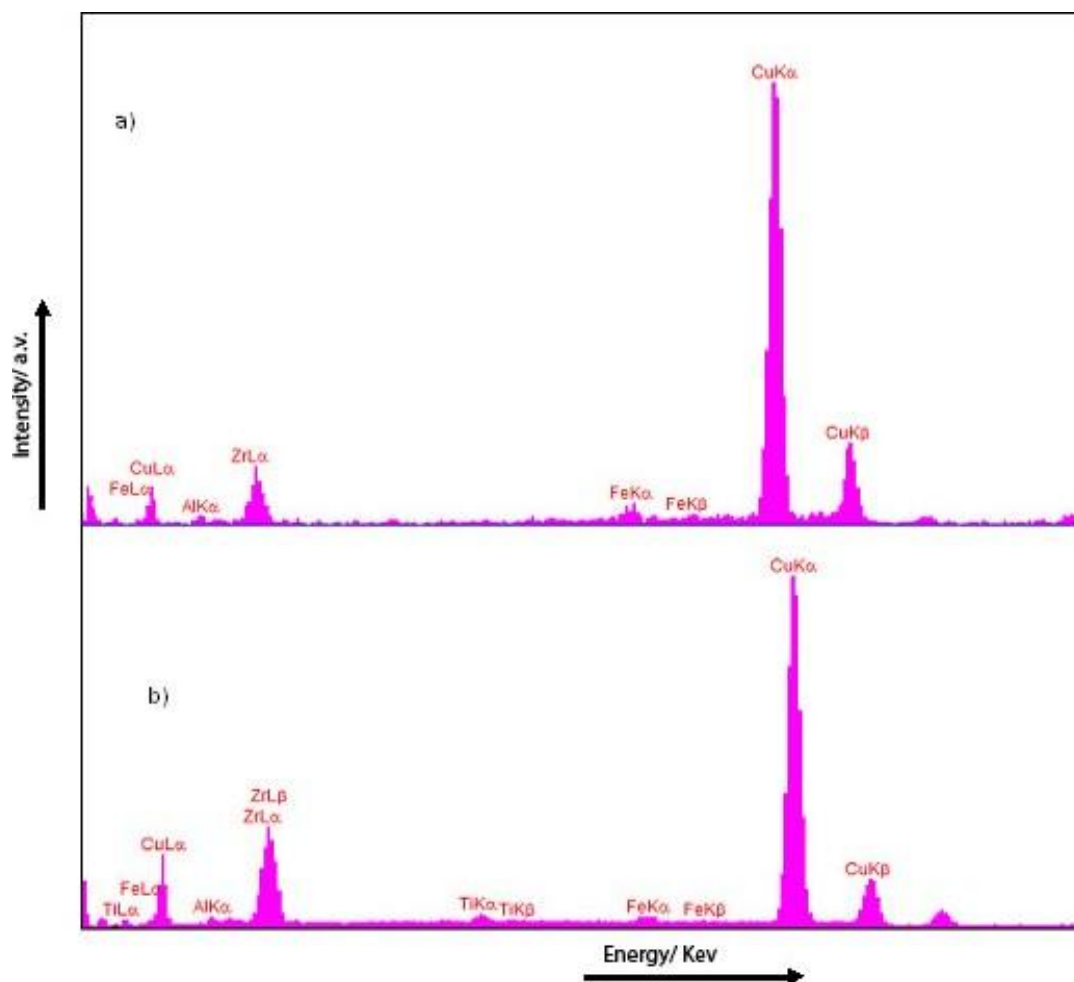


**Figure 4.** EDX results for (a)  $\text{Zr}_{60}\text{Cu}_{20}\text{Fe}_{10}\text{Al}_{10}$ , (b)  $\text{Zr}_{60}\text{Ti}_6\text{Cu}_{19}\text{Fe}_5\text{Al}_{10}$  BMGs.

Results showed that the Ti-bearing composition ( $\text{Zr}_{60}\text{Ti}_6\text{Cu}_{19}\text{Fe}_5\text{Al}_{10}$  BMG) increased the passive region ( $E_{\text{pit}} - E_{\text{corr}} = 0.70$ ) significantly. This is even higher compared to the SS 316L which is 0.472. SEM and EDX were employed to investigate the corroded surface morphologies and the chemical composition of corrosion precipitates in Zr-based BMGs. Fig. 3 shows the pits morphologies of the  $\text{Zr}_{60}\text{Cu}_{20}\text{Fe}_{10}\text{Al}_{10}$  and  $\text{Zr}_{60}\text{Ti}_6\text{Cu}_{19}\text{Fe}_5\text{Al}_{10}$  BMGs after the polarization. The insets in Fig. 3b,d exhibit the spongy (honeycomb mesh) structure for pits [15].

Fig. 4 shows the elemental composition of the pits in  $\text{Zr}_{60}\text{Cu}_{20}\text{Fe}_{10}\text{Al}_{10}$ ,  $\text{Zr}_{60}\text{Ti}_6\text{Cu}_{19}\text{Fe}_5\text{Al}_{10}$  BMGs. It is proved that corrosion pits initiate at weak spots of the passive films of the materials [20,22]. The weak spots could be linked to inclusions or physical defects in the passive films [22] but they actually cannot always be firmly recognized [23]. The growth mechanism of the pits in Zr-Cu-

based metallic glasses, once initiated, is not fully understood yet but Cu appears to play a strong role [15,20].

Fig. 4 shows that the level of Cu is higher in  $Zr_{60}Cu_{20}Fe_{10}Al_{10}$  (Fig. 4a) and  $Zr_{60}Ti_6Cu_{19}Fe_5Al_{10}$  (Fig. 4b) BMGs in comparison with other elements which shows Cu dissolved and redeposited in the pits [15]. This is clear since the standard half-cell potential of Cu is the nobler compared to Al, Zr, and Fe [24]. In fact when the potential increases the Cu dissolves but it would immediately redeposit into the pits to form the spongy (honeycomb mesh) structures [15].

It is reported that nano-crystallization process is supposed to occur by redeposit ion of dissolved Cu ions and the corrosion process is directly responsible for the formation of Cu nanocrystals because the crystallization takes place only inside the corroded areas [20]. Because Cu is the noblest element of the alloy, the deposition of Cu speeds up the dissolution of close regions of the material still rich in Zr, by forming a galvanic cell. Besides, Cu nano-crystals likely play a big role in corrosion morphology [20].

It is evidenced from Fig. 2 that  $Zr_{60}Cu_{22.5}Fe_{7.5}Al_{10}$  BMG, that has more Cu content than that of  $Zr_{60}Cu_{20}Fe_{10}Al_{10}$  BMG, shows more tendency to pitting corrosion when was compared to  $Zr_{60}Cu_{20}Fe_{10}Al_{10}$  BMG that can confirm Cu element effect on pitting corrosion. Optical microscopy image for surface of  $Zr_{60}Cu_{20}Fe_{10}Al_{10}$  BMG before electrochemical tests is shown in Fig. 5, which indicates the surface cracks on sample surface. It is reported that surface defects such as surface cracks which were created during casting or polishing are favorable sites for the intrusion of ions when samples were immersed in the electrolyte [15,24].

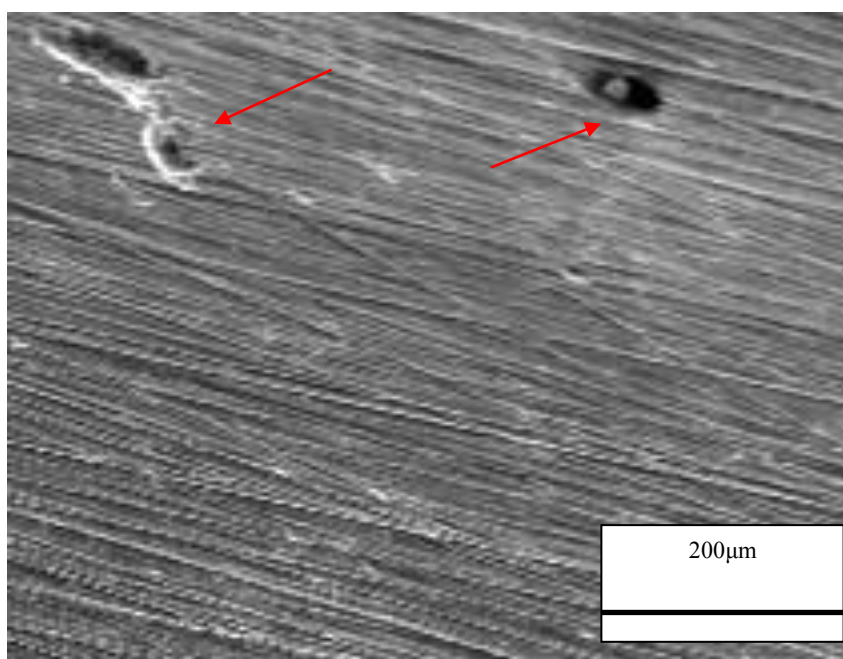


**Figure 5.** OM image for  $Zr_{60}Cu_{20}Fe_{10}Al_{10}$  BMG sample surface before anodic polarization (600-grit SiC surface finish).

On the other hand, our work showed that the addition of 6 atomic percents titanium improved the pitting corrosion resistance of Zr-Cu-Fe-Al BMGs. This is while the corrosion pits in  $Zr_{60}Ti_6Cu_{19}Fe_5Al_{10}$  are more but small compared to  $Zr_{60}Cu_{20}Fe_{10}Al_{10}$  (Fig. 3) that can indicate that the corrosion pits formed on  $Zr_{60}Ti_6Cu_{19}Fe_5Al_{10}$  BMG surface are more resistant to propagation. This could be the result of structural changes or acceleration in the passive film formation induced by titanium addition [25]. Thus, the structure and composition of surface passive film should be further studied to better understand the mechanisms concerning the effect of titanium addition on the  $Zr_{60}Ti_6Cu_{19}Fe_5Al_{10}$  BMG properties.

However, it is reported that none homogeneity within as-cast BMGs could result in localized imperfections in the surface passive film and lead to pitting corrosion [26]. Besides, the BMGs usually contain a certain amount of excess free volume (FV) which is created during quenching and is considered as a defect for an amorphous structure [4]. On the other hand, the excess FV is a metastable state and can be annihilated at the elevated temperature [4,27]. It is shown that by reducing the amount of FV in the glass, the passivation behavior is significantly improved [28]. Contact angle results for the BMGs are presented in Table 2. Contact angles become smaller than the Berg limit ( $\theta = 65^\circ$ ), which is beneficial for biomedical applications and can promote cell attachment on the surfaces of BMGs [29].

**Table 2.** Contact angles of water droplets measured on the BMGs

Composition	Contact Angle (Degree)
$Zr_{60}Cu_{22.5}Fe_{7.5}Al_{10}$	$58.9 \pm 1.3$
$Zr_{60}Cu_{20}Fe_{10}Al_{10}$	$53.0 \pm 1.7$
$Zr_{60}Ti_6Cu_{19}Fe_5Al_{10}$	$51.8 \pm 2.1$

Also, Table 2. Results demonstrated that Ti addition to Zr-Cu-Fe-Al BMGs slightly decreased contact angle and improved wettability. However, it is reported that surface finishing impresses surface wettability and affects cell behavior [30]. Lower cell adhesion and proliferation were found on smooth surfaces of Zr-based BMGs compared to their rougher counterparts [30].

#### 4. CONCLUSION

In this study  $Zr_{60}Cu_{22.5}Fe_{7.5}Al_{10}$ ,  $Zr_{60}Cu_{20}Fe_{10}Al_{10}$  and  $Zr_{60}Ti_6Cu_{19}Fe_5Al_{10}$  bulk metallic glasses were prepared by suction casting in copper mould.  $Zr_{60}Cu_{22.5}Fe_{7.5}Al_{10}$ ,  $Zr_{60}Cu_{20}Fe_{10}Al_{10}$  BMGs were spontaneously passivated and showed a quite low passive current densities in phosphate buffered solution. However, they were susceptible to pitting corrosion when compared to crystalline biomaterials. Results demonstrated that Ti addition to Zr-Cu-Fe-Al BMG system increased passive region significantly and improved pitting corrosion and surface wettability. Contact angle measurements showed that all the BMGs had Contact angles smaller than the Berg limit ( $\theta = 65^\circ$ ), which is beneficial for biomedical applications.

## ACKNOWLEDGMENTS

This work was funded by Tissue Engineering and Biomaterials Division of National Institute of Genetic Engineering and Biotechnology (Grant No: 440). We gratefully acknowledge the scientific assistance of Dr. R. Gholamipour and Dr. A.J. Gharebagh from Iranian Research Organization for Science and Technology (IROST) and technical assistance of M. Novin. We declare that we have no conflicts of interest.

## References

1. L. L. Hench, J. Jones, Biomaterials, Artificial Organs and Tissue Engineering, first ed., C.R.C, New York, 2005.
2. J. E. Ellingsen, S. P. Lyngstadaas, Bio-implant Interface: Improving Biomaterials and Tissue Reactions, first ed., C.R.C, New York, 2003.
3. B. D. Ratner, A. S. Hoffman, F. J. Schoen, J. E. Lemons, Biomaterials Science: An Introduction to Materials in Medicine, first ed., Academic, New York, 1996.
4. C. Suryanarayana , A. Inoue, Bulk Metallic Glasses, first ed., C.R.C, New York, 2011.
5. C. A. Schuh, T. C. Hufnagel , U. Ramamurty, *J. Acta Mater.* 55 (2007) 4067.
6. A. Inoue, X. M. Wang, W. Zhang, *J. Rev Adv Mater.* 18 (2008) 1.
7. J. Schroers, G. Kumar, T. M. Hodges , S. Chan, T. R. Kyriakides, *J. JOM.* 61 (2009) 21.
8. M. D. Demetriou, A. Wiest, D. C. Hofmann, W. L. Johnson, B. Han, N. Wolfson, et al., *J. JOM.* 62(2010) 83.
9. M. M. Trexler, N. N. Thadhani, *J. Prog Mater Sci.* 55 (2010) 759.
10. A. Inoue, A. Takeuchi, *J. Acta Mater.* 59 (2011) 2243.
11. C. J. Byrne, M. Eldrup, M. Ohnuma, R. S. Eriksen, *J. Mater Process Tech.* 210 (2010) 1419.
12. J. Schroers, T. Nguyen, S. O'Keefe, A. Desai, *J. Mater Sci Eng C.* 449-451 (2007) 898.
13. K. Kalimo, L. Mattila, H. Kautiainen, *J. Eur Acad Dermatol Venereol.* 18 (2004) 543.
14. Q. S. Zhang, W. Zhang, A. Inoue, *J. Scripta Mater.* 61 (2009) 241.
15. L. Huang, D. Qiao , B. A. Green, P. K. Liaw, J. Wang, S. Pang, et al., *J. Intermetallics.* 17 (2009)195.
16. L. Liu, C. L. Qiu, Q. Chen, S. M. Zhang, *J. Alloys and Compounds.* 425 (2006) 268.
17. Q. Chen, L. Liu, S. M. Zhang, *J. Front. Mater. Sci. China.* doi 10.1007/s11706-010-0004-5.
18. H.H. Huang, Y.S. Sun, C.P. Wu, C.F. Liu, P.K. Liaw, W. Kai, J. *Intermetallics*.doi:10.1016/j.intermet.2012.03.015
19. A. Gebert , P.F. Gostin, L. Schultz, *J. Corrosion Science.* 52 (2010) 1711.
20. J. Paillier, C. Mickel, P. F. Gostin, A. Gebert, *J. mat char.* 61 (2010) 1000.
21. X.P. Nie a, X.M. Xu b, Q.K. Jiang a, L.Y. Chen a, Y. Xua, Y.Z. Fang, et al., *J. Non- Cryst. Sol.* 355 (2009) 203.
22. J.R. Scully, A. Gebert, J.H. Payer, *J. Mater Res.* 22 (2007) 302.
23. B.A. Green, H.M. Meyer, R.S. Benson, Y. Yokoyama, P.K. Liaw, C.T. Liu. *J. Corros Sci.* 50 (2008)1825.
24. E.E. Stansbury, R.A. Buchanan , ASM International; 2000
25. Y.B. Wang, Y.F. Zheng, S.C. Wei, M. Li, *J. Biomed Mater Res B Appl Biomater.* 96 (2011) 34.
26. M. L. Morrison, R. A. Buchanan, A. Peker, W. H. Peter, J. A. Horton, P. K. Liaw. *J. Intermetallics,* 12 (2004) 1177.
27. W. Dmowski, C. Fan, M.L. Morrison, P.K. Liaw, T. Egami, *J. Mater Sci Eng A.* 471 (2007) 125.
28. J. Jayaraj, A. Gebert, L. Schultz, *J. Alloys Compd.* 479 (2009) 257.
29. Vogler E A, *J. Adv Colloid Interface Sci.* 74 (1998) 69.
30. L. Huang, Z. Cao, H.M. Meyer, P.K. Liaw, *J. Acta Biomater.* 7 (2011) 395.